Macromolecules

Article

pubs.acs.org/Macromolecules

Charge-Regulated Spontaneous, Reversible Self-Assembly of the Carboxylic Acid-Functionalized Hydrophilic Fullerene Macroanions in Dilute Solution

Panchao Yin, Zhiwei Lin, Jiayingzi Wu, Chih-Hao Hsu, Xinyue Chen, Jing Zhou, Pengtao Lu, Seyed Ali Eghtesadi, Xinfei Yu, Stephen Z. D. Cheng,* and Tianbo Liu*

Department of Polymer Science, The University of Akron, Akron, Ohio 44325-3909, United States

Supporting Information

ABSTRACT: Fullerene molecule covalently functionalized with 12 carboxylic acid groups on its periphery was synthesized, and its solution behavior was explored. The functionalized fullerene molecules behave as hydrophilic macroions in polar solvents by showing strong attractions with each other mediated from their counterions and consequently self-assembling into single-layer, hollow, spherical blackberry-type structures in solvents with moderate polarity. The fullerene molecules are not touching with each other in the assemblies, and the assembly size can be tuned by changing the polarity of the solvents. More importantly, the transition between the self-assembly and the disassembly of the macroions can be easily achieved by changing temperature. The discovery confirms that the semirigid clusters demonstrate the unique solution behavior of macroions and open up a new way to assemble fullerene into functional materials and devices.

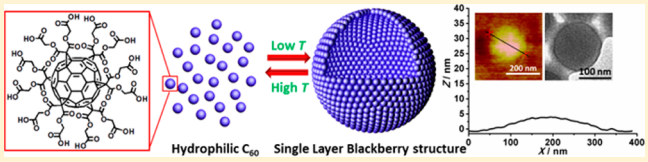

INTRODUCTION

The fullerene, with its important and amazing molecular structure,[1,2] excellent electronic properties,[3−5] and appreciable medical applications,[6,7] has been leading to continuous and extensive attentions in many different fields since its discovery in 1985.[8] Assembling fullerenes, in particular, their derivatives, into hierarchical ordered structures across multilength scales represents one of the most popular protocols in processing fullerene into functional materials and devices.[9−13] Noncovalent interactions, including hydrogen bonding,[14−16] hydrophobic interactions,[17,18] and aromatic stacking,[12,19,20] are the most common driving forces for the assembly of fullerene derivatives. Therefore, a thorough understanding of the roles of noncovalent interactions playing in their self-assembly behavior is quite critical in designing the fullerene derivatives and programming them into required morphologies and functions,[21] as proved by the continuous efforts from different groups on investigating the self-assembly of fullerene derivatives driven by single or multiple types of noncovalent interactions.[22−26] In particular, as a class of most intensively studied fullerene derivatives, the amphiphilic fullerenes provide a versatile platform for engineering controllable assemblies of fullerene derivatives in solution and in the bulk.[22,24,27−30] Rich phase behaviors and abundant hierarchically ordered structures have been shown from the self-assembly of various amphiphilic fullerenes involving driving forces such as hydrogen bonding, hydrophobic interaction, and aromatic stacking.[19,21−38]

However, surprisingly, the study of the fully hydrophilic, highly charged fullerenes in their solutions is completely missing. Electrostatic interaction is expected to be dominant in such solutions. The self-assembly of hydrophilic fullerenes associating with electrostatic interactions is not only of scientific interest to creating new hierarchical structures without the involvement of hydrophobic interaction but also of practical importance to paving a way for relevant applications. In this paper we demonstrate our new effort on understanding the solution behavior of hydrophilic, charged fullerenes, particularly on applying simple electrostatic interactions to achieve their spontaneous, reversible, and size controllable assembly, with the help of our previous understanding on hydrophilic macroionic solutions. The solution chemistry of macroions, a group of highly charged molecules/particles at nanoscale, represents a new regime in solution chemistry between simple ionic solutions and colloidal suspensions.[39−42] These macroions, including but not limiting to polyoxometalates, metal−organic cationic nanocages, and some biomacromolecules, demonstrate unique solution behaviors by self-assembling into single layer, hollow, spherical assemblies (coined by us with the name "blackberry" structures), which is obviously different from small simple ions.[39,40,43] These macroions cannot be treated as insoluble colloidal suspensions because they form stable real solutions.[39,40] The synthesis of highly charged and symmetrical hydrophilic fullerenes provides perfect models for expanding the study of macroions by pushing the size limit of macroions to ca. 1.5 nm and other types of compounds/clusters.[44] Moreover, the "soft" layer of the hydrophilic fullerene molecules not only provides convenience for processing them into devices but also serves as analogue of

Received: November 2, 2014
Revised: January 7, 2015
Published: January 16, 2015

DOI: 10.1021/ma5022314
Macromolecules 2015, 48, 725−731

the soft matter nature of biomacromolecules.[45,46] The deprotonation of carboxylic groups results in the high charge on the fullerene molecules, sharing the similarity of negative charged polymers and biomacromolecules. On the other hand, a thorough study of solution behavior of these highly charged hydrophilic fullerenes could open a new way to achieve unique ordered structures beyond those from traditional fullerene derivatives. Herein, we report the studies of the solution behavior of 12 carboxylic acid group-capped fullerene (AC_{60}) in organic solvents and in water by using laser light scattering (LLS), TEM, and AFM techniques.

EXPERIMENTAL SECTION

Synthesis of the Carboxylic Acid Functionalized Fullerene Molecules. The synthesis of targeted hydrophilic fullerene (AC_{60}) by installing 12 carboxylic acid groups on the periphery of fullerene molecule was achieved based on the procedures described in the previous publications.[30,47] Despite the reported procedures, the chemical characterizations of AC_{60} and the corresponding important intermediate compounds (tC_{60}) have not yet been provided previously. To ensure the well-defined structures and high purities of as-prepared AC_{60}, the chemical structures of tC_{60} and AC_{60} were fully characterized by ^{1}H NMR, ^{13}C NMR, and MALDI-TOF mass spectra (see section 2 of Supporting Information). In the mass spectrum of tC_{60} (Figure S1), only one strong peak exists, where the monoisotopic mass peak observed at m/z = 2701.1 agrees well with the calculated value (2700.8). The deprotection of *tert*-butyl groups on hydrophobic tC_{60} to afford hydrophilic AC_{60} is unambiguously evidenced by the complete disappearance of *tert*-butyl protons at 1.45 ppm in the ^{1}H NMR spectrum as well as the *tert*-butyl carbons at 28.2 and 82.9 ppm in the ^{13}C NMR spectrum. In particular, the appearance of sp^3 carbon atoms at 68.7 ppm and the two different types of sp^2 carbon atoms at 140.8 and 145.7 ppm suggest T_h symmetry of carbon cage, validating precisely defined structures of AC_{60}.[48,49]

Static Light Scattering. The functionalized fullerene samples were fully dissolved in required solvent with the help of stirring and sonication. The obtained solution was then filtered to a precleaned 20 mL vial by passing the solution through a 500 nm filter. The filtered solution was ready for both DLS and SLS studies. The concentrations of the assemblies were determined by UV−vis measurements (see section 6 of Supporting Information). A commercial Brookhaven Instrument LLS spectrometer equipped with a solid-state laser operating at 532 or 637 nm was used for measurement of both SLS and DLS. SLS experiments were performed at scattering angles (θ) between 20° and 120°, at 2° intervals. However, due to the large fluctuations in scattered intensities at low scattering angles, we removed the data from 20° to 40° in the final analysis. Derived from Rayleigh−Gans−Debye equation,[50] a Zimm plot was used to analyze the SLS data to obtain the radius of gyration (R_g) and molecular weight (M_w) of the assemblies.

Dynamic Light Scattering. DLS measures the intensity−intensity time correlation function by means of a BI-9000AT multichannel digital correlator. The field correlation function $|g^{(1)}(\tau)|$ was analyzed by the constrained regularized CONTIN method[51] to yield information on the distribution of the characteristic line width Γ from $|g^{(1)}(\tau)| = \int G(\Gamma)e^{-\Gamma\tau}\,d\Gamma$. The normalized distribution function of the characteristic line width, $G(\Gamma)$, so obtained, can be used to determine an average apparent translational diffusion coefficient, $D_{app} = \Gamma/q^2$. The hydrodynamic radius (R_h) is related to D via the Stokes−Einstein equation: $R_h = kT/(6\pi\eta D)$, where k is the Boltzmann constant and η the viscosity of the solvent at temperature T. From DLS measurements, we can obtain the particle-size distribution in solution from a plot of $\Gamma G(\Gamma)$ versus R_h. The R_h of the particles is obtained by extrapolating $R_{h,app}$ to zero scattering angle.

Transmission Electron Microscopy. 20 μL of the AC_{60} assembly solution was carefully titrated on the surface of one copper grid. The excess solution was then quickly wicked away by filter paper. The copper grid containing samples was then allowed to dry under ambient conditions. The bright-field images were recorded on a digital CCD camera in JEOL-1230 microscope with an accelerating voltage of 120 kV.

Atomic Force Microscopy. AFM experiments were carried out on a Dimension Icon AFM (Bruker AXS). Samples were prepared by depositing 30 μL of AC_{60} assembly solution in THF onto the silicon wafer and drying under ambient conditions. The images were obtained at the scanning rate of 0.5 Hz in the tapping mode over 1.2 × 1.2 μm^2.

RESULTS AND DISCUSSION

Synthesis and Molecular Structure. C_{60} is regiospecifically functionalized with 12 carboxylic acid groups on periphery of six symmetric active sites through the Bingel−Hirsch cyclopropanation reaction[52−55] (Figure 1). Structural study of

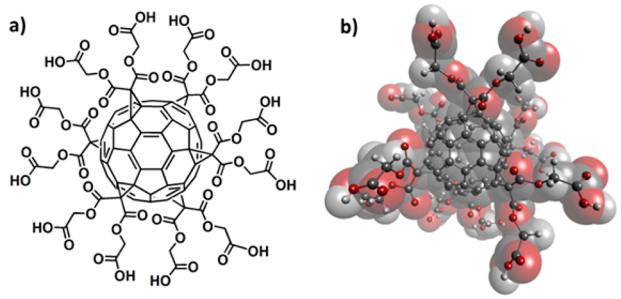

Figure 1. Chemical structure (a) and ball−stick model (b) of the AC_{60} molecule. The ball−stick model is built based on DFT optimization. Color code of spheres: gray, C; white, H; red, O.

the AC_{60} molecular structure after DFT optimization and the dynamic analysis of the soft chain indicate that the size of the molecule is ca. 1.5 nm (section 3 in Supporting Information). The anchored carboxylic acid groups make AC_{60} an almost fully hydrophilic molecule, which cannot be dissolved in nonpolar solvent, e.g. toluene, but can be soluble in polar solvents and water (at high pH). The AC_{60} molecules can only be dissolved in water with pH > 11.2 to achieve the concentration 0.5 mg/mL since they carry more charges at a higher pH. Dynamic light scattering (DLS) measurements on aqueous solution (pH ∼ 13.0) of AC_{60} indicate the existence of particles with size as ca. 1.3 nm, which is consistent with the structural analysis results (Figure S6 in Supporting Information) that the AC_{60} clusters exist as discrete anions in aqueous solution.

Self-Assembly Behavior of the AC_{60} Molecules. The AC_{60} molecules are quite soluble in THF to achieve as high concentration as ca. 1.30 mg/mL. The scattered intensity at 90° for the freshly prepared THF solution of AC_{60} (0.65 mg/mL) is very low, at 8.5 kcps (scattered intensity for benzene is ca. 69 kcps), suggesting that almost all AC_{60} exist as monomers. Time-resolved static light scattering (SLS) measurement on this solution shows a continuous, significant increase of scattered intensity with time, indicating the self-assembly of AC_{60} molecules into supramolecular structures. The overall intensity growth shows a sigmoid-shape kinetic curve. The self-assembly process shows a lag phase of 4 days and reaches equilibrium in ca. 40 days (Figure 2a) at room temperature.[56,57] A typical CONTIN analysis[51] of dynamic light scattering (DLS) measurements of the solution indicates the formation of larger structures with an average hydrodynamic radius (R_h) of 95 ± 5 nm with no angular dependence (Figure 2b). No obvious change of the assembly size is observed during the whole self-assembly process, suggesting it is the number of the assemblies,

DOI: 10.1021/ma5022314
Macromolecules 2015, 48, 725−731

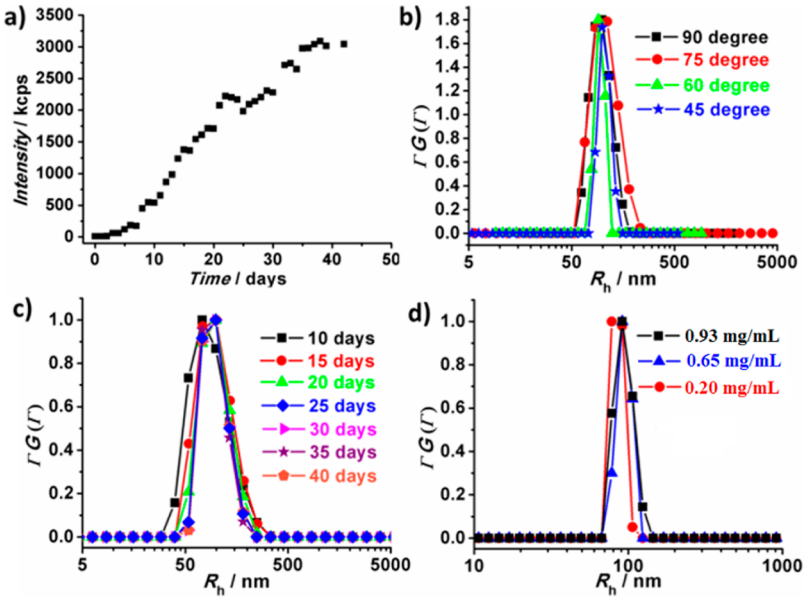

Figure 2. (a) Time-resolved SLS measurements of 0.65 mg/mL AC_{60} in THF at 90° scattering angle. (b) CONTIN analysis of the DLS data of 0.65 mg/mL AC_{60} in THF solution (on the 40th day) at different scattering angles. (c) CONTIN analysis of time-resolved DLS data of 0.65 mg/mL AC_{60} in THF at 90° scattering angle. (d) CONTIN analysis of DLS data of AC_{60} in THF solutions with different concentrations (0.93, 0.65, and 0.20 mg/mL, 40th day) at scattering angle of 60°.

not the size of the assemblies, that increases with time during the assembly process (Figure 2c).[56,57] DLS study of other two THF solutions of the AC_{60} molecules with different concentration (0.93 and 0.20 mg/mL, respectively) shows that the average R_h value of the assemblies are 91 ± 5 and 85 ± 5 nm, respectively, indicating that the size of the formed assemblies is concentration-independent (Figure 2d). Zimm plot fitting[58] of the SLS measurements of the assemblies (Figure 3a) in the above three solutions indicates that radius of gyration (R_g) of the assemblies is 90 ± 5 nm, which is very close to their R_h values (95 ± 5 nm). The $R_g \sim R_h$ result suggests that hollow, spherical assemblies are formed in THF, which is also confirmed by bright-field TEM observations shown in Figure 3b. The wall thickness of the assemblies was measured to be ca. 2 nm from this TEM image (the dark ring circles at the outmost sides of the assemblies). Since the dimension of AC_{60} molecules is around 1.5 nm, it is proposed that the assemblies are constructed by a single-layered molecular packing, as schematically illustrated in Figure 3c. Further analysis of the Zimm plot indicates that the average molecular weight of the assemblies is ca. 1.44×10^5 kDa, corresponding to around 76 000 AC_{60} molecules for each assembly. Since the sizes of the AC_{60} and the assemblies are known, it is straightforward to draw the conclusion that the assemblies are single-layer hollow spherical structure (section 6 in Supporting Information); that is, AC_{60} molecules are likely to form "blackberry" structures instead of forming bilayer surfactant-like vesicles. To further validate the single-layered model, the layer thicknesses of the collapsed assemblies after slowly evaporating the solvent were characterized by the atomic force microscopy (AFM). As the typical height profile of two assemblies exhibited in Figure 3d, the average thickness of assemblies was measured to be 4.0 ± 0.5 nm from 10 independent measurements, which is in good agreement with the theoretical double thicknesses of AC_{60} molecules (ca. 3 nm) of the collapsed "blackberry" model (Figure 3e and section 7 in Supporting Information). The double-layered vesicles have

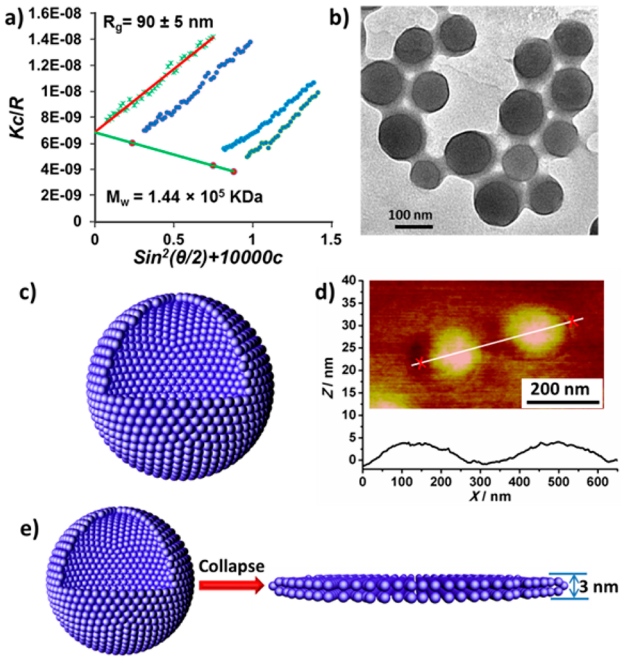

Figure 3. (a) Zimm plot of three AC_{60}/THF solutions with different concentrations (0.93, 0.65, and 0.20 mg/mL). (b) TEM images of the assemblies from the AC_{60}/THF solution (0.65 mg/mL). (c) Schematic illustration of single layer hollow spherical structure formed by AC_{60} in THF (each blue sphere represents one AC_{60} molecule). (d) AFM height profile of collapsed assemblies after solvent evaporation. Inset is typical AFM image of two individual assemblies. (e) Schematic illustration of collapsed single-layer hollow spherical assembly model.

been generally achieved by the assembly of fullerene-based amphiphiles,[19,22−24] yet no example has been demonstrated to form single-layered hollow spherical structures from fullerene-based derivatives. Thus, this work might provide a new and facile strategy to control the generation of single-layered assemblies of fullerenes and their derivatives.

DOI: 10.1021/ma5022314
Macromolecules 2015, 48, 725−731

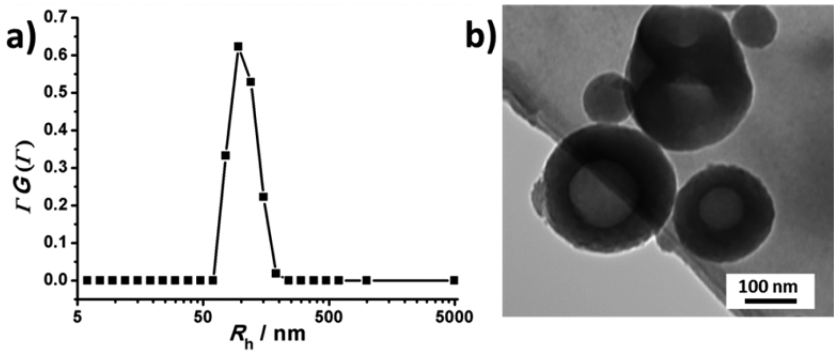

Figure 4. (a) CONTIN analysis of DLS data of the AC_{60}/HFIP solution (0.5 mg/mL) at scattering angle as 90°. (b) TEM image of the assemblies in the AC_{60}/HFIP solution (0.5 mg/mL).

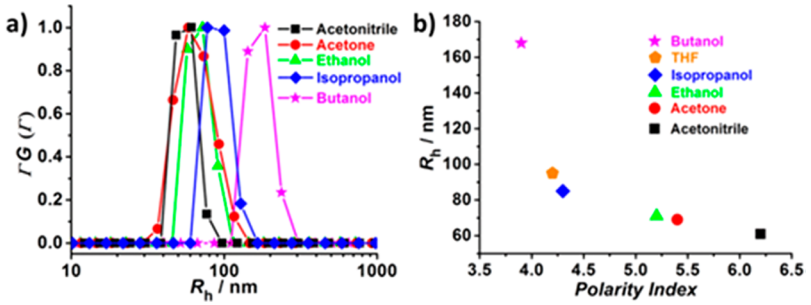

Figure 5. (a) CONTIN analysis of the DLS data of 0.5 mg/mL AC_{60} in various solvents at scattering angles as 90°. (b) Summary of the R_h value of the assemblies vs the polarity index of the corresponding solvents including acetonitrile, acetone, ethanol, isopropanol, THF, and *n*-butanol.

Mechanism of the Self-Assembly. The self-assembly mechanism is investigated by studying the solution behavior of AC_{60} in solvents with different polarities. Time-resolved SLS studies confirmed that the self-assembly process, suggested from the high scattered intensities, was observed in the solutions of acetone, acetonitrile, ethanol, isopropanol, and *n*-butanol (Figure S7). However, the AC_{60} molecules are soluble in DMF, DMSO, methanol, and water (at pH > 11.2) without forming larger assemblies, indicated by the very low scattered intensities of corresponding solutions (Figure S5). The latter group of solvents is actually solvents with higher polarities than the former group. It is acknowledged that the high polarity of solvent environment favors the hydrophobic interaction-driven self-assembly process. Therefore, the above observation rules out the possibility that hydrophobic interaction is the driving force for the self-assembly of AC_{60} in solution. The structure of this fully hydrophilic AC_{60} molecule does not provide any domain for hydrophobic interaction either.

Meanwhile, hydrogen-bonding interaction is also excluded as the major driving force for such self-assembly process. The AC_{60} molecules are observed to self-assemble in alcohols, including ethanol, isopropanol, and *n*-butanol, implying that hydrogen bonding might not be the major driving force for the self-assembly process since the abundance of alcohol molecules could terminate the intermolecular hydrogen bonding of AC_{60}. Moreover, the solution behavior of the AC_{60} was further studied in hexafluoro-2-propanol (HFIP). HFIP is a polar solvent and a hydrogen donor, which enable it to dissolve substances and serve as hydrogen bond cutting agent.[59] However, the formation of vesicular assemblies with sizes as ca. 200 nm are observed in LLS and TEM results, providing strong evidence to rule out hydrogen bonding as the major driving force (Figure 4).

Counterion-mediated attraction is expected to be the main driving force for the self-assembly process. It is believed that the carboxylic acid groups are able to partially deprotonated, and therefore, the AC_{60} molecules are charged in polar solvents, which can be regarded as typical microanions. Polarity index (PI), defined as a measure of the ability of the solvent to interact with various test solutes, is key parameter of the indication of solvent polarity.[60] Herein, PI can be used to estimate the interaction between the solvent molecules and the solute of carboxylic acid-capped fullerenes. The interaction will directly lead to the deprotonation of the carboxylic acid groups. The amount of charge AC_{60} carries relies on the degree of deprotonation (α) of the capped carboxylic acid groups, which could be estimated based on FT-IR results. The value of α could at least qualitatively indicate the degree of deprotonation. Obviously, the AC_{60} possesses a much higher α value in DMF (ca. 62%)[61] and methanol (ca. 47%) than that in THF (ca. 19%) (section 8 in Supporting Information). It is observed that the AC_{60} macroanions are able to self-assemble in organic solvent with medium polarities (e.g., THF), not able to self-assemble in solvents with high polarities (e.g., methanol). Because of the different deprotonation degree of −COOH groups in the solvents, the carboxylic acid groups shelled AC_{60} are highly charged in solvents with high polarities, which could surpass the charge density limit in forming "blackberry" structures.[40,62,63] Further analysis indicates that the assembly sizes become larger in solvents with lower polarity indexes, which is consistent with previous theories of counterion mediated attraction (Figure 5 and Figure S9 of Supporting Information).[40,62,63] The deprotonating degree of −COOH group is higher in solvents with higher polarity index value, and therefore the surface charge density of AC_{60} becomes too high, which decreases the attraction among the monomers and lead

DOI: 10.1021/ma5022314
Macromolecules 2015, 48, 725−731

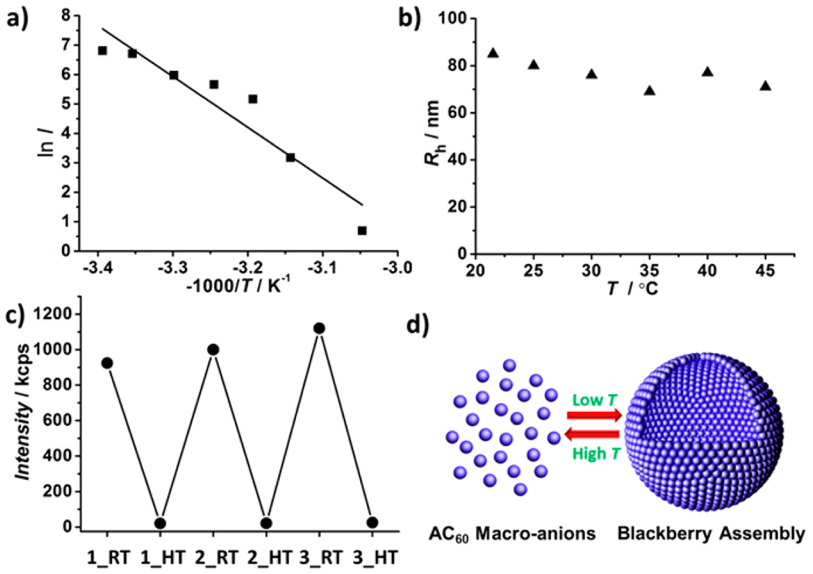

Figure 6. (a) ln I vs $-1/T$ data of the thermodynamic study of the isopropanol solution of the AC_{60} and the linear fit curve of the data. The linear fitting results: $y = -17258x - 51.02$. (b) The R_h value of assemblies in the isopropanol solution of the AC_{60} vs the corresponding solution temperature. (c) The reversible process of "blackberry" self-assembly/disassembly process by monitoring the scattered intensity of AC_{60}/isopropanol solution at 90° scattering angle while the temperature was equilibrated at room temperature (RT, 21.5 °C) and high temperature (HT, 55 °C). (d) Graphic representation of the reversible self-assembly/disassembly process of "blackberry".

to a larger curvature, e.g., smaller sizes for "blackberry" structures.

It is worthy to note that the AC_{60} macroanions are able to self-assemble in acetonitrile, however, not in acetic acid despite the identical polarity index of these two solvents (Figure S8 in Supporting Information). The deprotonation of −COOH shelled on the AC_{60} core relies on not only the polarity of the organic solvent but also other features of the solvent. Acetic acid provides abundant carboxylic groups in the AC_{60} solution, which will significantly inhibit the deprotonation of AC_{60}. Therefore, AC_{60} exists as neutral molecules in acetic acid, making counterion-induced attraction impossible.

Thermodynamics of the Self-Assembly Process. The time-resolved SLS monitoring of the solutions of AC_{60} at different temperatures could provide information on the stability of the assemblies and the thermodynamics of the self-assembly process. It is suggested from our previous results that the individual macroions and their assemblies coexist in equilibrium state in the solutions.[64,65] The counterion-mediated interaction and possible hydrogen bonding contribute to the self-assembly. Raising temperature can accelerate the self-assembly process of macroions.[65] However, no study has been carried out so far to investigate the temperature effect on the thermodynamics of the self-assembly process.

SLS measurements on 0.5 mg/mL AC_{60} in isopropanol indicates that the scattered intensity at 90° scattering angle decreases as the temperature increases stepwise from room temperature to 60 °C. DLS studies of the same solution indicate that the R_h value of the assemblies does not change noticeably during the temperature-changing process. This suggests that the number of the assemblies in solution is decreasing while their sizes do not change when the temperature increases (Figure 6a,b). The scattered intensity at 60 °C is comparable to the intensity of the AC_{60}/isopropanol solution without assemblies, suggesting that tiny amount of assemblies exist while most of the assemblies disassemble at higher temperature. The scattered intensity I is used to estimate the equilibrium constant. The ln I vs $-1/T$ linear fitting curve can be used to qualitatively estimate the enthalpy and entropy changes (ΔH and ΔS) of the "blackberry" formation process (Figure 6, and section 9 in Supporting Information). Both the slope and intercept values of the linear regression are negative, suggesting that both ΔH and ΔS are negative for such a self-assembly process. The self-assembly is exothermal and entropy decreasing, and therefore, there should be a critical temperature, at which the Gibbs free energy (ΔG) becomes zero and the self-assembly is not favored. Further quantitative analysis of the thermodynamic results can be used to calculate the disassembly temperature for the above systems. Since the solution scattered intensity I is proportional to the concentration of the assemblies, there exists the relation $\ln k \sim B \ln I$ with B being constant. For the change of Gibbs free energy of the assembly process, $\Delta G = \Delta H - T\Delta S = -RT \ln k \sim -BRT \ln I$. Therefore, $\Delta S/BR - (\Delta H/BR)(1/T) \sim \ln I$. By fitting the plot of ln I vs $-1/T$, two parameters can be obtained: slope = $\Delta H/BR$; intercept = $\Delta S/BR$. At the critical temperature, $\Delta G = \Delta H - T_c\Delta S = 0$. Therefore

$$T_c = \Delta H/\Delta S = \frac{\text{slope}}{\text{intercept}} = 338.26\ \text{K} \sim 65\ ^\circ\text{C} \quad (1)$$

The critical temperature is calculated to be ca. 338 K (65 °C) based on the ratio of slope and intercept of the linear function shown in Figure 6a, in excellent agreement with our experimental results above. Interestingly, the scattered intensity of this AC_{60}/isopropanol solution increases back to its original value when the solution temperature tunes back to room temperature, proving that such temperature-controlled assembly/disassembly process is reversible. Another two of such temperature-control cycles have been observed, and similar self-assembly/disassembly behaviors are confirmed (Figure 6c,d). This is the first time the transition between "blackberry" assemblies and single macroanion has been achieved by changing temperatures.

DOI: 10.1021/ma5022314
Macromolecules 2015, 48, 725−731

Similar temperature-dependent self-assembly experiment is carried out with 0.5 mg/mL AC_{60}/acetonitrile solution. The scattered intensity at 90° scattering angle decreases to half of its original value when the temperature is increased from room temperature to 65 °C (Figure S12). The scattered intensity is back to high value when the solution temperature is back to room temperature (Figure S12). The observation is consistent with the above conclusion on the thermodynamics of "blackberry" formation. The assemblies would completely disassemble into monomeric AC_{60} macroanions in isopropanol at 65 °C while only around 50% of the assemblies disassemble in acetonitrile. The AC_{60} macroanions can interact with isopropanol through the hydrogen bonding from the interaction between −COOH of AC_{60} and −OH of isopropanol. Compared to acetonitrile, isopropanol favors to dissolve AC_{60} at individual anion level. Therefore, the assemblies of AC_{60} macroanions could be easier to be broken into monomers in isopropanol.

CONCLUSION

In summary, a hydrophilic fullerene derivative (AC_{60}) with 12 carboxylic acid groups shelled on the periphery shows the behavior of macroions by self-assembling into single-layer "blackberry" structures. Its solution behavior is different from previous amphiphilic fullerenes. The size of the assemblies is inversely dependent on the polarity of the solvent. The major driving force is confirmed to be counterion-mediated attraction. The self-assembly and disassembly of AC_{60} in solutions have been proved to be reversible via temperature. Our protocol provides a new way to assemble fullerene derivatives into ordered vesicular structures with tunable sizes and narrow size distribution and might afford a feasible strategy to the design and preparation of single-layered structures based on fullerene and their derivatives.

ASSOCIATED CONTENT

Supporting Information

More experimental details and Figures S1−S12. This material is available free of charge via the Internet at http://pubs.acs.org.

AUTHOR INFORMATION

Corresponding Authors

*E-mail tliu@uakron.edu (T.L.).
*E-mail scheng@uakron.edu (S.Z.D.C.).

Author Contributions

P.Y. and Z.L. contributed equally to this work.

Notes

The authors declare no competing financial interest.

ACKNOWLEDGMENTS

T. Liu acknowledges support from the NSF (CHE1306505) and the University of Akron. S.Z.D.C. acknowledges support from National Science Foundation (DMR-1408872). The authors also acknowledge Yan Sun and Prof. Alamgir Karim for the assistance in AFM experiments and Jie Yu and Prof. Steven Chuang for helping FT-IR tests and analyses.

REFERENCES

(1) Krätschmer, W.; Lamb, L. D.; Fostiropoulos, K.; Huffman, D. R. *Nature* **1990**, *347*, 354−358.
(2) Bühl, M.; Hirsch, A. *Chem. Rev.* **2001**, *101*, 1153−1183.
(3) Guldi, D. M.; Illescas, B. M.; Atienza, C. M.; Wielopolskia, M.; Martín, N. *Chem. Soc. Rev.* **2009**, *38*, 1587−1597.
(4) Dresselhaus, M. S.; Dresselhaus, M.; Eklund, P. C. *Science of Fullerenes and Carbon Nanotubs*; Academic Press: San Diego, CA, 1996.
(5) Roncali, J. *Chem. Soc. Rev.* **2005**, *34*, 483−495.
(6) Jensen, A. W.; Wilson, S. R.; Schuster, D. I. *Bioorg. Med. Chem.* **1996**, *4*, 767−779.
(7) Bosi, S.; Da Ros, T.; Spalluto, G.; Prato, M. *Eur. J. Med. Chem.* **2003**, *38*, 913−923.
(8) Kroto, H. W.; Heath, J. R.; O'Brien, S. C.; Curl, R. F.; Smalley, R. E. *Nature* **1985**, *318*, 162−163.
(9) Nakanishi, T. *Chem. Commun.* **2010**, *46*, 3425−3436.
(10) Nakanishi, T.; Ariga, K.; Michinobu, T.; Yoshida, K.; Takahashi, H.; Teranishi, T.; Möhwald, H.; Kurth, D. G. *Small* **2007**, *3*, 2019−2023.
(11) Babu, S. S.; Möhwald, H.; Nakanishi, T. *Chem. Soc. Rev.* **2010**, *39*, 4021−4035.
(12) Sawamura, M.; Kawai, K.; Matsuo, Y.; Kanie, K.; Kato, T.; Nakamura, E. *Nature* **2002**, *419*, 702−705.
(13) Liu, Y.; Zhang, G.; Niu, L.; Gan, L.; Liang, D. *J. Mater. Chem.* **2011**, *21*, 14864−14868.
(14) Arias, F.; Godínez, L. A.; Wilson, S. R.; Kaifer, A. E.; Echegoyen, L. *J. Am. Chem. Soc.* **1996**, *118*, 6086−6087.
(15) Sánchez, L.; Rispens, M. T.; Hummelen, J. C. *Angew. Chem., Int. Ed.* **2002**, *41*, 838−840.
(16) Xiao, S.; Li, Y.; Fang, H.; Li, H.; Liu, H.; Shi, Z.; Jiang, L.; Zhu, D. *Org. Lett.* **2002**, *4*, 3063−3066.
(17) Nakanishi, T.; Michinobu, T.; Yoshida, K.; Shirahata, N.; Ariga, K.; Möehwald, H.; Kurth, D. G. *Adv. Mater.* **2008**, *20*, 443−446.
(18) Nakanishi, T.; Miyashita, N.; Michinobu, T.; Wakayama, Y.; Tsuruoka, T.; Ariga, K.; Kurth, D. G. *J. Am. Chem. Soc.* **2006**, *128*, 6328−6329.
(19) Cassell, A. M.; Asplund, C. L.; Tour, J. M. *Angew. Chem., Int. Ed.* **1999**, *38*, 2403−2405.
(20) Matsuo, Y.; Muramatsu, A.; Hamasaki, R.; Mizoshita, N.; Kato, T.; Nakamura, E. *J. Am. Chem. Soc.* **2004**, *126*, 432−433.
(21) Guldi, D. M.; Zerbetto, F.; Georgakilas, V.; Prato, M. *Acc. Chem. Res.* **2005**, *38*, 38−43.
(22) Zhou, S.; Burger, C.; Chu, B.; Sawamura, M.; Nagahama, N.; Toganoh, M.; Hackler, U. E.; Isobe, H.; Nakamura, E. *Science* **2001**, *291*, 1944−1947.
(23) Homma, T.; Harano, K.; Isobe, H.; Nakamura, E. *J. Am. Chem. Soc.* **2011**, *133*, 6364−6370.
(24) Homma, T.; Harano, K.; Isobe, H.; Nakamura, E. *Angew. Chem., Int. Ed.* **2010**, *49*, 1665−1668.
(25) Yu, X.; Zhang, W.-B.; Yue, K.; Li, X.; Liu, H.; Xin, Y.; Wang, C.-L.; Wesdemiotis, C.; Cheng, S. Z. D. *J. Am. Chem. Soc.* **2012**, *134*, 7780−7787.
(26) Muñoz, A.; Illescas, B. M.; Sánchez-Navarro, M.; Rojo, J.; Martín, N. *J. Am. Chem. Soc.* **2011**, *133*, 16758−16761.
(27) Georgakilas, V.; Pellarini, F.; Prato, M.; Guldi, D. M.; Melle-Franco, M.; Zerbetto, F. *Proc. Natl. Acad. Sci. U. S. A.* **2002**, *99*, 5075−5080.
(28) Liu, B.; Yang, M.; Zhang, Z.; Zhang, G.; Han, Y.; Xia, N.; Hu, M.; Zheng, P.; Wang, W. *Langmuir* **2010**, *26*, 9403−9407.
(29) Zhang, W.-B.; Yu, X.; Wang, C.-L.; Sun, H.-J.; Hsieh, I.-F.; Li, Y.; Dong, X.-H.; Yue, K.; Van Horn, R.; Cheng, S. Z. D. *Macromolecules* **2014**, *47*, 1221−1239.
(30) Yu, X.; Yue, K.; Hsieh, I.-F.; Li, Y.; Dong, X.-H.; Liu, C.; Xin, Y.; Wang, H.-F.; Shi, A.-C.; Newkome, G. R.; Ho, R.-M.; Chen, E.-Q.; Zhang, W.-B.; Cheng, S. Z. D. *Proc. Natl. Acad. Sci. U. S. A.* **2013**, *110*, 10078−10083.
(31) Brettreich, M.; Burghardt, S.; Böttcher, C.; Bayerl, T.; Bayerl, S.; Hirsch, A. *Angew. Chem., Int. Ed.* **2000**, *39*, 1845−1848.
(32) Burghardt, S.; Hirsch, A.; Schade, B.; Ludwig, K.; Böttcher, C. *Angew. Chem., Int. Ed.* **2005**, *44*, 2976−2979.

DOI: 10.1021/ma5022314
Macromolecules 2015, 48, 725−731

(33) Lin, Z.; Lu, P.; Hsu, C.-H.; Yue, K.; Dong, X.-H.; Liu, H.; Guo, K.; Wesdemiotis, C.; Zhang, W.-B.; Yu, X.; Cheng, S. Z. D. *Chem.—Eur. J.* **2014**, *20*, 11630−11635.
(34) Dai, S.; Ravi, P.; Tan, C. H.; Tam, K. C. *Langmuir* **2004**, *20*, 8569−8575.
(35) Ravi, P.; Wang, C.; Dai, S.; Tam, K. C. *Langmuir* **2006**, *22*, 7167−7174.
(36) Wang, C.; Ravi, P.; Tam, K. C. *Langmuir* **2006**, *22*, 2927−2930.
(37) Wang, C.; Ravi, P.; Tam, K. C. *Langmuir* **2007**, *23*, 8798−8805.
(38) Ravi, P.; Dai, S.; Tan, C. H.; Tam, K. C. *Macromolecules* **2005**, *38*, 933−939.
(39) Liu, T. *Langmuir* **2010**, *26*, 9202−9213.
(40) Yin, P.; Li, D.; Liu, T. *Chem. Soc. Rev.* **2012**, *41*, 7368−7383.
(41) Yin, P.; Zhang, J.; Li, T.; Zuo, X.; Hao, J.; Warner, A. M.; Chattopadhyay, S.; Shibata, T.; Wei, Y.; Liu, T. *J. Am. Chem. Soc.* **2013**, *135*, 4529−4536.
(42) Liu, T.; Langston, M. L. K.; Li, D.; Pigga, J. M.; Pichon, C.; Todea, A. M.; Müller, A. *Science* **2011**, *331*, 1590−1592.
(43) Liu, T.; Diemann, E.; Li, H.; Dress, A. W. M.; Müller, A. *Nature* **2003**, *426*, 59−62.
(44) Zhou, J.; Yin, P.; Hu, L.; Haso, F.; Liu, T. *Eur. J. Inorg. Chem.* **2014**, 4593−4599.
(45) Mishra, P. P.; Pigga, J.; Liu, T. *J. Am. Chem. Soc.* **2008**, *130*, 1548−1549.
(46) Zhang, J.; Li, D.; Liu, G.; Glover, K. J.; Liu, T. *J. Am. Chem. Soc.* **2009**, *131*, 15152−15159.
(47) Lin, Z.; Lu, P.; Yu, X.; Zhang, W.-B.; Huang, M.; Wu, K.; Guo, K.; Wesdemiotis, C.; Zhu, X.; Zhang, Z.; Yue, K.; Cheng, S. Z. D. *Macromolecules* **2014**, *47*, 4160−4168.
(48) Iehl, J.; de Freitas, R. P.; Delavaux-Nicot, B.; Nierengarten, J.-F. *Chem. Commun.* **2008**, 2450−2452.
(49) Iehl, J.; Nierengarten, J.-F. *Chem. Commun.* **2010**, *46*, 4160−4162.
(50) Hiemenz, P. C.; Rajagopalan, R. *Principles of Colloid and Surface Chemistry*; Marcel Dekker: New York, 1997.
(51) Provencher, S. W. *Comput. Phys. Commun.* **1982**, *27*, 229−242.
(52) Bingel, C. *Chem. Ber.* **1993**, *126*, 1957−1959.
(53) Hirsch, A.; Vostrowsky, O. *Eur. J. Org. Chem.* **2001**, 829−848.
(54) Hirsch, A.; Lamparth, I.; Grösser, T.; Karfunkel, H. R. *J. Am. Chem. Soc.* **1994**, *116*, 9385−9386.
(55) Hirsch, A.; Lamparth, I.; Karfunkel, H. R. *Angew. Chem., Int. Ed.* **1994**, *33*, 437−438.
(56) Liu, T. *J. Am. Chem. Soc.* **2002**, *124*, 10942−10943.
(57) Liu, T. *J. Am. Chem. Soc.* **2003**, *125*, 312−313.
(58) Zimm, B. H. *J. Chem. Phys.* **1948**, *16*, 1099−1116.
(59) Siegemund, G.; Schwertfeger, W.; Feiring, A.; Smart, B.; Behr, F.; Vogel, H.; McKusick, B. In *Ullmann's Encyclopedia of Industrial Chemistry*; Wiley-VCH Verlag GmbH & Co. KGaA: Weinheim, 2000.
(60) Reichardt, C.; Welton, T. *Solvents and Solvent Effects in Organic Chemistry*, 4th ed.; Wiley-VCH Verlag GmbH & Co. KGaA: Weinheim, 2010.
(61) Yu, X.; Zhong, S.; Li, X.; Tu, Y.; Yang, S.; Van Horn, R. M.; Ni, C.; Pochan, D. J.; Quirk, R. P.; Wesdemiotis, C.; Zhang, W.-B.; Cheng, S. Z. D. *J. Am. Chem. Soc.* **2010**, *132*, 16741−16744.
(62) Liu, T.; Imber, B.; Diemann, E.; Liu, G.; Cokleski, K.; Li, H.; Chen, Z.; Müller, A. *J. Am. Chem. Soc.* **2006**, *128*, 15914−15920.
(63) Kistler, M. L.; Bhatt, A.; Liu, G.; Casa, D.; Liu, T. *J. Am. Chem. Soc.* **2007**, *129*, 6453−6460.
(64) Li, D.; Zhou, W.; Landskron, K.; Sato, S.; Kiely, C. J.; Fujita, M.; Liu, T. *Angew. Chem., Int. Ed.* **2011**, *50*, 5182−5187.
(65) Liu, G.; Liu, T. *Langmuir* **2005**, *21*, 2713−2720.

DOI: 10.1021/ma5022314
Macromolecules 2015, 48, 725−731